Demonstration of the Density Dependence of X-Ray Flux in a Laser-Driven Hohlraum

P. E. Young, M. D. Rosen, J. H. Hammer, W. S. Hsing, S. G. Glendinning, R. E. Turner, R. Kirkwood, J. Schein,[*] C. Sorce,
J. H. Satcher, Jr., A. Hamza, R. A. Reibold, R. Hibbard, O. Landen, and A. Reighard

University of California, Lawrence Livermore National Laboratory, P. O. Box 808, Livermore, California 94550, USA

S. McAlpin, M. Stevenson, and B. Thomas

Atomic Weapons Establishment, Aldermaston, Reading, United Kingdom RG7 4PR
(Received 11 April 2008; published 14 July 2008)

Experiments have been conducted using laser-driven cylindrical hohlraums whose walls are machined from Ta_2O_5 foams of 100 mg/cc and 4 g/cc densities. Measurements of the radiation temperature demonstrate that the lower density walls produce higher radiation temperatures than the high density walls. This is the first experimental demonstration of the prediction that this would occur [M. D. Rosen and J. H. Hammer, Phys. Rev. E **72**, 056403 (2005)]. For high density walls, the radiation front propagates subsonically, and part of the absorbed energy is wasted by the flow kinetic energy. For the lower wall density, the front velocity is supersonic and can devote almost all of the absorbed energy to heating the wall.

Present designs for laser-driven inertial confinement fusion (ICF) use capsules that are either driven directly by laser pulses or indirectly by converting the laser pulses to x-rays in a hohlraum target. The conventional indirect ICF target consists of a solid density gold shell or hohlraum that surrounds the capsule [1]. The amount of x-ray radiation available depends on the initial conversion efficiency of laser light into primary x-rays and on the x-ray reemission efficiency of the hohlraum walls. Research continues to investigate methods of improving the amount of x-rays that reach the capsule [2]. This research is significant because improvements in target performance mean increased operating margins for a given laser capability.

One approach that has been proposed [3] is to manufacture the hohlraum walls from a gold foam whose average density is less than solid gold. This is possible because, for a certain density range, less of the x-ray energy goes into energy lost into the wall compared to solid density walls, so that the balance can be reemitted onto the capsule. Gold foams are predicted to decrease the amount of lost energy by ~17% [3].

In this Letter, we report on experiments that demonstrate for the first time the predicted density dependence of the hohlraum wall loss. The wall density is varied by manufacturing hohlraums made of tantalum oxide (Ta_2O_5) foams of two different densities. We will begin by summarizing the theoretical basis of the target design, discuss the targets, laser and diagnostics used. The experimental results are then described and compared to the theoretical prediction.

Laser irradiation of the hohlraum wall produces primary x-rays that act as a heat source and create a nearly blackbody radiation field inside the hohlraum. The radiation is lost to the capsule, out of the laser entrance holes, and to the walls of the hohlraum. The x-ray radiation heats the walls of the hohlraum and creates a radiation front, or Marshak wave [4,5], that propagates into the wall. The change in the wall energy, E, per unit area A, is given by

$$E/A \approx \rho e X_M, \qquad (1)$$

where ρ is the wall density, e is the internal energy per unit mass, and X_M is the propagation distance of the Marshak wave.

The distance X_M has been determined from analytic solutions [5] of the radiation diffusion equation

$$\rho \frac{\partial e}{\partial t} = \frac{4}{3} \frac{\partial}{\partial x} \left(\frac{1}{K\rho} \frac{\partial \sigma T^4}{\partial x} \right), \qquad (2)$$

where T is the temperature, and K is the Rosseland mean opacity. We assume the functional forms $e = fT^\beta \rho^{-\mu}$ and $K = g^{-1}T^{-\alpha}\rho^\lambda$, where α, β, μ, and λ are fit to tabulated values for the selected wall material. For the materials discussed in this Letter, $\alpha \approx 1.5$, $\beta \approx 1.6$, $\mu \approx 0.14$, and $\lambda \approx 0.2$.

The solution for Eq. (2) has been found to depend on the initial wall density [3]. For wall densities near solid density, the radiation front velocity is subsonic. In this case, the energy is absorbed in a small layer at the surface of the wall, creating sufficiently high pressure to ablate the wall and create a plasma. At high density, we expect X_M to be relatively independent of the initial wall density because the Marshak wave only sees the ablation density profile.

For sufficiently low wall densities, the Marshak wave velocity is supersonic so the density can be assumed to be constant in time and space. The solution [3,5] in this case for gold gives

$$X_M = 0.0012 T^{1.95} \tau^{0.5} / \rho^{1.03} \text{ (cm)} \qquad (3)$$

so, from Eq. (1),

$$E/A = 0.0029T^{3.55}\tau^{0.5}/\rho^{0.17} \ (\text{MJ/cm}^2). \quad (4)$$

Thus, the density dependence of Eq. (4) is due primarily to the density dependence of e. From Eq. (3) one can see that, at low density, as ρ increases, the velocity, $\dot{X}_M$, decreases, so, while the front still proceeds supersonically, a larger fraction of the tail of the radiation wave profile develops a rarefaction wave. Thus, Eq. (4) must include a term that takes into account the increase in kinetic energy due to that rarefaction wave

$$E/A = 0.0029T^{3.55}\tau^{0.5}/\rho^{0.17}$$
$$+ 0.0035\rho^{0.79}T^{2.4}\tau \ (\text{MJ/cm}^2). \quad (5)$$

This last equation has a minimum when

$$\rho^* = 0.17T_{heV}^{1.2}t_{ns}^{-0.5} \ \text{g/cc}. \quad (6)$$

When substituted back into Eq. (5), this ρ^* gives an E/A lower by 17% than the subsonic case [3], where the rarefaction kinetic energy plays an even bigger role throughout the radiation front. This presents the opportunity to reduce the hohlraum wall loss by constructing the hohlraum wall with a low-density foam.

We have performed experiments that confirm the theoretical predictions. We chose Ta_2O_5 as the material for the hohlraum walls, because of the relative ease of producing mechanically stable foams of two densities (100 mg/cc and 4 g/cc) different enough to produce an observable difference in x-ray flux. Foams of 100 mg/cc density are readily available using an aerogel process [6], and we expect, from Eq. (6), that the energy loss to the wall is near a minimum at this density when $T \sim 100$ eV. High density foams can be formed by pressing and sintering Ta_2O_5 particles to achieve a density of 4 g/cc. The predicted difference in wall loss for 4 g/cc foam compared to solid density is only $\sim 1\%$.
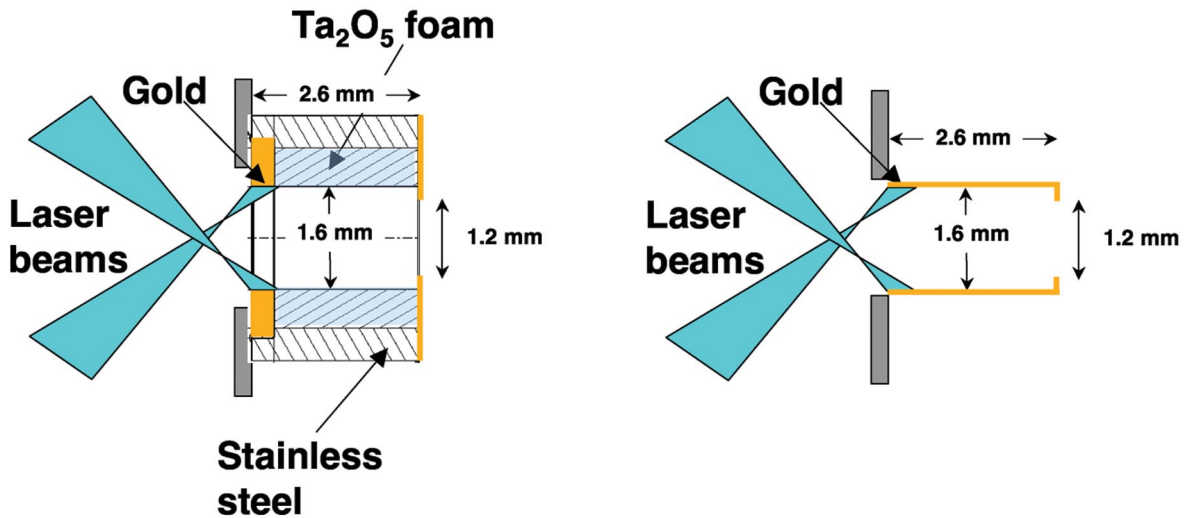
Balancing the x-ray source energy to the x-ray energy sinks of wall loss and hole loss, and invoking the predicted difference in wall loss between the 100 mg/cc and the 4 g/cc foam for $T \approx 100$ eV of 13%, leads to a predicted T difference, δT of ~ 2.5 eV. The *observed* δT will be larger due to the difference in the wall albedo, α, where

$$\alpha = F_{rad}/F_{inc} = 1 - (F_{abs}/F_{inc}) = 1 - (F_{abs}/\sigma T^4). \quad (7)$$

F_{inc} is the x-ray flux in the hohlraum cavity, F_{abs} is the flux absorbed in the wall, and F_{rad} is the flux reradiated by the wall. Combining the facts that the absorbed flux in 4 g/cc Ta_2O_5 foam is 20% higher than that of gold, with $F_{abs} = \dot{E}_{abs}/A$, and the subsonic solution for the Marshak wave at solid density gold, leads to [2,5]

$$\alpha_s = 1 - 1.2 \times (0.34/T^{0.7}) = 0.60. \quad (8)$$

The 100 mg/cc foam has 13% lower wall loss than the high density foam so

$$\alpha_f = 1 - 0.87 \times 1.2 \times (0.34/T^{0.7}) = 0.65. \quad (9)$$

Applying the correction

$$T_{obs} = T_w \alpha^{1/4} = 102.5 \ \text{eV} \times (0.65/0.60)^{0.25} = 104 \ \text{eV} \quad (10)$$

we obtain a temperature difference for the two densities in excellent agreement with the computation predictions and the experimental results.

For our experimental design, we chose a hohlraum that is illuminated from one end with 15 laser beams (see Fig. 1), and whose axis is oriented so that the flux diagnostic (Dante) can view the x-ray emittance of the hohlraum wall at an angle of 41.8° from the hohlraum axis without seeing the laser spots. Dante is a multichannel time-resolved x-ray spectrometer with a demonstrated absolute accuracy of ±5% [7]. Each channel is filtered to

FIG. 1 (color).   (a) Design and dimensions of the foam-walled Ta_2O_5 hohlraum targets. (b) Design and dimensions of the solid gold hohlraum targets.

maximize transmission for a given energy band from 50 eV to 2.5 keV. The $T \sim 100$ eV of the targets discussed here is covered by the 5 lowest energy channels which utilize grazing incidence mirrors to reject the high energy x rays that make it through the filters. The x rays are detected by x-ray diodes (XRDs) whose signal is recorded by a fast transient scope. The time response of the XRD and scope is approximately 140 ps.

The hohlraum was irradiated with 15 beams of the Omega laser that were positioned on a ring of solid gold in order to have a source of primary x rays that is independent of the foam density. The beams were chosen to have an incident angle at the ring of less than 45°: 6 beams had an incident angle of 42.2°, 3 had an incidence angle of 31.2°, and 6 beams had an incidence angle of 27.7°. Each beam produced approximately 350 J of 0.35-μm light in a

1-ns reverse ramp (RR1001) pulse. The pulse shape was chosen to keep T approximately constant during the laser pulse, as is assumed by the theory. Elliptical phase plates were used to spatially smooth the laser intensity profile at the hohlraum wall.

The given amount of laser energy and the design temperature of 100 eV led to a hohlraum with an inner diameter of 1.6 mm and a length of 2.6 mm (see Fig. 1). The hohlraum was formed by first either casting the 100 mg/cc foam, or pressing and sintering Ta_2O_5 particles into a stainless steel form, then machining out the center to form a foam cylinder. The end of the hohlraum facing the Dante diagnostic was covered with a gold washer of 1.2 mm diameter. This washer further obscured the laser spots from the Dante field of view and also covered the
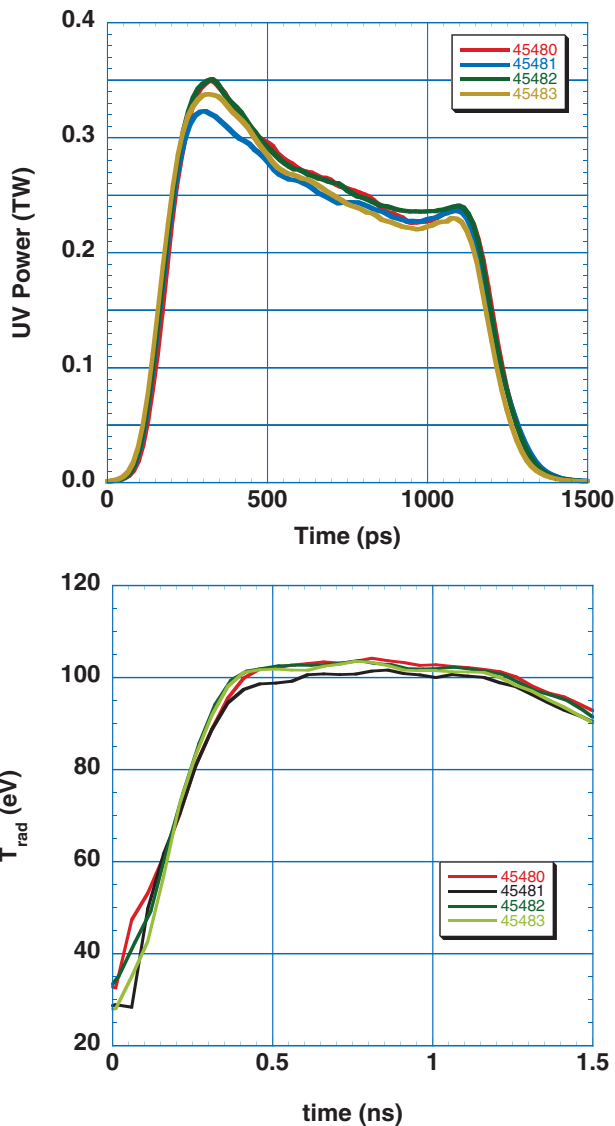

FIG. 2 (color).   (a) Average laser pulse for 15 beams used in the solid gold hohlraums. (b) Radiation temperature from Dante measurement for four solid gold hohlraums.
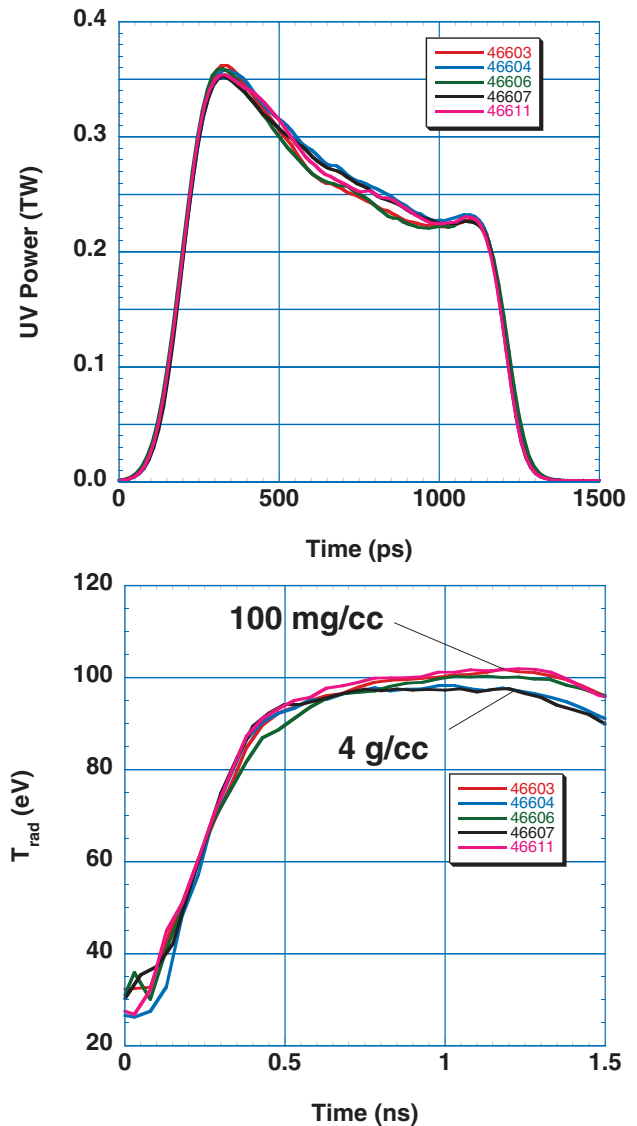
FIG. 3 (color).   (a) Average laser pulse for 15 beams used in the foam hohlraums. (b) Radiation temperature from Dante measurement for five foam hohlraums.
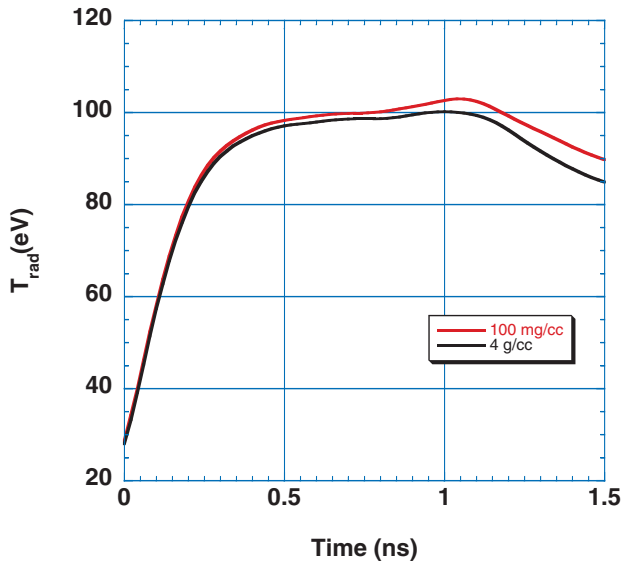
FIG. 4 (color).   Calculated radiation temperature for the two foam densities.

exposed end of the foam so the propagating radiation front did not change the emission area viewed by Dante.

The unfold of the radiation temperature from the Dante signals requires knowledge of the emission area, which can change over time if material is ablated from the inside of the observation hole. To measure the emission area as a function of time, an x-ray framing camera was used with a soft x-ray (SXR) imaging snout. The emission source is imaged with a pinhole through a mirror-filter pair that define the wavelength band at which the image is obtained. For this experiment, we used three channels, (i) Ge mirror at 3° incidence and a 1 μm Zn filter (450 eV), (ii) Al mirror at 3° incidence and a 1 μm V filter (760 eV) and (iii) a 1 mil-thick Be filter (<1.5 keV). No measurable closure of the Dante viewing hole was observed while the laser was on.

We compare results between experiments performed over an 8 h period. The channel response of the spectrometer can change if the filters are damaged or coated with target debris. The spectrometer performance was monitored by alternating the foam density on each shot; we observed that the Dante measurements were very reproducible for each of the two foam densities. Also, the filters were inspected after the shot series to verify that there was no significant increase in filter pinhole area or observable coatings.

To measure the shot-to-shot reproducibility of the Dante signal, we shot 4 identical solid gold hohlraums with the same inner dimensions as the foam hohlraums [see Fig. 1(b)]. The average laser energy is 5.6 kJ $\pm$ 300 J (summed over 15 beams); i.e., the shot-to shot variation is ~5%. Figure 2(b) shows the radiation temperature deconvolved from Dante signals from four separate experi-

ments; the maximum difference is ~1 eV at any given time.

Data from the foam hohlraum shots is shown in Fig. 3. Again the pulse shape and energy is highly reproducible over the course of five shots. The radiation temperature is clearly higher for the lower foam density, with a temperature that is higher by ≈ 4 eV (corresponding to an flux increase of ~17%), all in agreement with the analytic prediction.

The observed density dependence of the radiation temperature agrees with the predictions of 2D simulations, as well. The simulation results using the Lagrangian NYM code [8] are shown in Fig. 4. Both the density dependence and the time history of the radiation temperature agree well with the experimental measurements, and are independently duplicated by the LLNL 2D code LASNEX.

In summary, we have demonstrated, for the first time, increased radiation temperature in foam-walled hohlraums when compared to solid density walls. The Ta foam results presented here motivate development of gold foams. For $T_{\rm rad} \sim 250$ eV, the optimum density is 400 mg/cc.

*Present address: Labor für Plasmatechnik, Universität der Bundeswehr München, Werner-Heisenberg-Weg 39, D-85577 Neubiberg, Germany.

[1] J. Lindl, *Inertial Confinement Fusion* (Springer-Verlag, New York, 1998).

[2] M. D. Rosen, in *Proceedings of the Scottish University Summer School in Physics 2005 on High Energy Laser-Matter Interactions*, edited by D. Jaroszynsky (Taylor & Francis, CRC Press, London, 2005); M. D. Rosen, in *Proceedings of the 33rd EPS Conference on Plasma Physics*, edited by F. DeMarco and G. Vlad (EPS Publishers, Frascati, Italy, 2006), Vol. 30I, p. 2006.

[3] M. D. Rosen and J. H. Hammer, Phys. Rev. E **72**, 056403 (2005).

[4] R. E. Marshak, Phys. Fluids **1**, 24 (1958).

[5] J. H. Hammer and M. D. Rosen, Phys. Plasmas **10**, 1829 (2003).

[6] T. F. Baumann, A. E. Gash, G. A. Fox, J. H. Satcher, Jr., and L. W. Hrubesh, in *Handbook of Porous Materials* (Wiley-VCH, Weinheim, 2002).

[7] C. Sorce, J. Schein, F. Weber, K. Widmann, K. Campbell, E. Dewald, R. Turner, O. Landen, K. Jacoby, P. Torres, and D. Pellinen, Rev. Sci. Instrum. **77**, 10E518 (2006).

[8] P. D. Roberts, S. J. Rose, P. C. Thompson, and R. J. Wright, J. Phys. D **13**, 1957 (1980).